Am J Physiol Heart Circ Physiol 309: H615–H624, 2015.
First published June 12, 2015; doi:10.1152/ajpheart.00246.2015.

Mechanical support of the pressure overloaded right ventricle: an acute feasibility study comparing low and high flow support

Tom Verbelen,[1] Jelle Verhoeven,[1] Motohiko Goda,[1] Daniel Burkhoff,[2] Marion Delcroix,[3] Filip Rega,[1] and Bart Meyns[1]

[1]*Department of Cardiac Surgery, University Hospitals Leuven and Department of Cardiovascular Sciences, University of Leuven, Leuven, Belgium;* [2]*Division of Cardiology, Columbia University College of Physicians and Surgeons, New York, New York; and* [3]*Respiratory Division, University Hospitals Leuven and Department of Clinical and Experimental Medicine, University of Leuven, Leuven, Belgium*

Submitted 6 April 2015; accepted in final form 11 June 2015

Verbelen T, Verhoeven J, Goda M, Burkhoff D, Delcroix M, Rega F, Meyns B. Mechanical support of the pressure overloaded right ventricle: an acute feasibility study comparing low and high flow support. *Am J Physiol Heart Circ Physiol* 309: H615–H624, 2015. First published June 12, 2015; doi:10.1152/ajpheart.00246.2015.—The objectives of this study were to assess the feasibility of low flow right ventricular support and to describe the hemodynamic effects of low versus high flow support in an animal model of acute right ventricular pressure overload. A Synergy Pocket Micro-pump (HeartWare International, Framingham, MA) was implanted in seven sheep. Blood was withdrawn from the right atrium to the pulmonary artery. Hemodynamics and pressure-volume loops were recorded in baseline conditions, after banding the pulmonary artery, and after ligating the right coronary artery in these banded sheep. End-organ perfusion (reflected by total cardiac output and arterial blood pressure) improved in all conditions. Intrinsic right ventricular contractility was not significantly impacted by support. Diastolic unloading of the pressure overloaded right ventricle (reflected by decreases in central venous pressure, end-diastolic pressure and volume, and ventricular capacitance) was successful, but with a concomitant and flow-dependent increase of the systolic afterload. This unloading diminished with right ventricular ischemia. Right ventricular mechanical support improves arterial blood pressure and cardiac output. It provides diastolic unloading of the right ventricle, but with a concomitant and right ventricular assist device flow-dependent increase of systolic afterload. These effects are most distinct in the pressure overloaded right ventricle without profound ischemic damage. We advocate the low flow strategy, which is potentially beneficial for the afterload sensitive right ventricle and has the advantage of avoiding excessive increases in pulmonary artery pressure when pulmonary hypertension exists. This might protect against the development of pulmonary edema and hemorrhage.

pressure overloaded right ventricle; mechanical support; partial support

NEW & NOTEWORTHY

Mechanically supporting the pressure overloaded right ventricle improves arterial blood pressure and cardiac output and provides diastolic unloading, but with concomitant and right ventricular assist device flow-dependent increases of systolic afterload. The low flow strategy benefits the afterload sensitive right ventricle and avoids excessive increases in pulmonary pressures. This might protect against pulmonary hemorrhage and pulmonary edema.

Address for reprint requests and other correspondence: T. Verbelen, Dept. of Cardiac Surgery, Univ. Hospitals Leuven, Herestraat 49, 3000 Leuven, Belgium (e-mail: tom.verbelen@med.kuleuven.be).

MEDICAL MANAGEMENT OF RIGHT ventricular failure (RVF) includes inotropic support to enhance right ventricular (RV) contractility, pulmonary vasodilation to reduce RV afterload, and volume resuscitation to maintain RV preload (19). Surgical treatment of acute RVF refractory to this medical treatment remains challenging. The most commonly used options include catheter-based RV assist devices (RVADs) (TandemHeart; Impella RP), venoarterial extracorporeal membrane oxygenation, heart transplantation, and, rarely, atrial septostomy (10). Right-sided use of left ventricular (LV) assist devices (LVADs) has mainly been used in the context of RVF post-LVAD implantation but also in patients with biventricular failure, RV infarction, post-cardiotomy RVF, and RVF following heart transplantation (4, 9, 10, 20–22).

Increased pulmonary vascular resistance (PVR) is an important contributing factor in many patients with RVF. In such cases, RV support with devices that provide relatively high flow rates might result in increased pulmonary pressures and lung injury, whereas left atrial filling and cardiac output (CO) would remain low (1). However, recently developed smaller mechanical circulatory assist devices with lower flow capacities might be more appropriate for RV support. The concept of low flow (partial) ventricular support with the Synergy Micropump has already been shown to result in significant hemodynamic benefits in appropriately selected cases of LV failure (17, 18). Accordingly, this system has been proposed for use in patients with RVF due to pressure overload (22).

As a first step in the feasibility testing of low flow mechanical support of the pressure overloaded RV, we aimed to assess the hemodynamic effects of low versus high flow mechanical support in an animal model of acute RV pressure overload with and without ischemic failure.

MATERIAL AND METHODS

Animal preparation. This study was approved by the KULeuven animal ethics committee (P127/2011). All animals received humane care in compliance with the Principles of Laboratory Animal Care formulated by the National Society for Medical Research and the *Guide for the Care and Use of Laboratory Animals* prepared by the Institute of Laboratory Animal Resources (National Institutes of Health). Seven ewe (Swifter-Charolais) of 45.2 ± 5.2 kg, aged 10.5 ± 0.8 mo, were included. After sedation with 15 mg/kg intramuscular ketamine, anesthesia was induced with isoflurane. The sheep were positioned in a right lateral position. After intubation, the animals were mechanically ventilated with the use of a volume-controlled respirator (Dräger, Cicero). Anesthesia was maintained with isoflurane (2% to 3%) in a gas mixture consisting of 80–100% oxygen supplemented with room air. The ruminant stomach was decompressed with a 12-bore orogastric

tube. Anesthesia was monitored by checking eyelid reflexes and continuous monitoring throughout the study of end tidal CO_2 (respiratory volume and frequency were adapted to keep it within ranges of 35–45 mmHg), ECG, arterial blood pressure (ABP), heart rate, and blood O_2 saturation. Buprenorphine-hydrochloride (0.3 mg) and Meloxicam (0.5 mg/kg iv) were used for analgesia.

Instrumentation. Figure 1 shows a schematic overview of the experimental setup. Pressure lines in the left ear artery and the left jugular vein served to measure ABP and central venous pressure (CVP), respectively. A Swan-Ganz catheter was introduced in the left jugular vein, and by fluoroscopic guidance the tip was placed in the distal pulmonary trunk for measuring distal pulmonary artery pressure (PAP). A left thoracotomy through the fourth intercostal space was performed, and the heart was exposed in a pericardial cradle. The aorto-pulmonary window was dissected, and a band was loosely placed around the distal pulmonary trunk. A Synergy Micro-pump (HeartWare International, Framingham, MA) was inserted to withdraw blood from the right atrium (RA) to the pulmonary artery (PA). A Sono TT flowmeter (Emtec, Gennevilliers, France) around the tubing system of the pump measured pump flow. A TS420 flowmeter (Transonic Systems Europe B.V., Maastricht, The Netherlands) around the proximal PA, proximal to the outflow graft of the pump measured the CO generated by the RV (RVCO). Pressure lines in the left atrium, in the PA between the pulmonary valve and the Transonic flowmeter, and just proximal to the band served to measure left atrial pressure (LAP), proximal PAP, and PAP just proximal to the band, respectively. Finally, a 7F combined pressure-conductance catheter was connected to a Sigma M signal processor (both CD Leycom, Zoetermeer, The Netherlands). After pressure calibration, this catheter was positioned in the RV through a stab wound just below the pulmonary valve and positioned toward the apex for continuous and simultaneous measurement of pressure and volume. RV parallel conductance was determined by using hypertonic saline injections, and the slope factor α was assessed by comparing the uncalibrated conductance catheter CO with the CO obtained by the Transonic flowmeter.

Following hemodynamic assessments under baseline conditions (baseline), two experimental conditions mimicking the effects of acute RV pressure overload were created. In the first case, pressure overload was induced by tightening a band around the PA distal to the pump outflow tract, as much as was hemodynamically tolerated (banding). In the second case, the right coronary artery was ligated in these banded sheep (banding + ischemia). Ten minutes after establishing each of these three experimental conditions, pressures, flows, and a pressure-volume (PV)-loop were recorded at zero pump speed, at low flow (22,000 rpm), and at high flow (28,000 rpm) in all sheep. Finally, the sheep were euthanized by means of injection of 20 ml KCl (14.9%) after reassurance of adequate anesthesia.

The Synergy Micro-pump. This system was originally designed for partial LV support (17). The micro-pump was connected to an inflow cannula with an intra-atrial cage, an outflow graft, and an electrical lead connected to the external controller and power supply. As an LVAD, this micro-pump can provide up to 4.25 l of blood flow per minute.

Data analysis. Total CO was calculated by adding intrinsic RVCO and pump flow. The ratio of pump flow/total CO represents the fraction of augmented blood flow generated by the RVAD. RV power was calculated as mean proximal PAP*pulmonary flow*0.0022 and total power as mean PAP just before the banding*total CO*0.0022. PV-loop analysis was performed using CD Leycom and Matlab R2013a (MathWorks, Natick, MA) software. In each beat, end systole was defined as the point in the cardiac cycle of maximal $P(t)/V(t)$, where $P(t)$ is the instantaneous RV pressure and $V(t)$ is the instantaneous RV volume. Stroke work (SW) was calculated as the PV loop area for each beat. The pressure-volume area (PVA) represents the

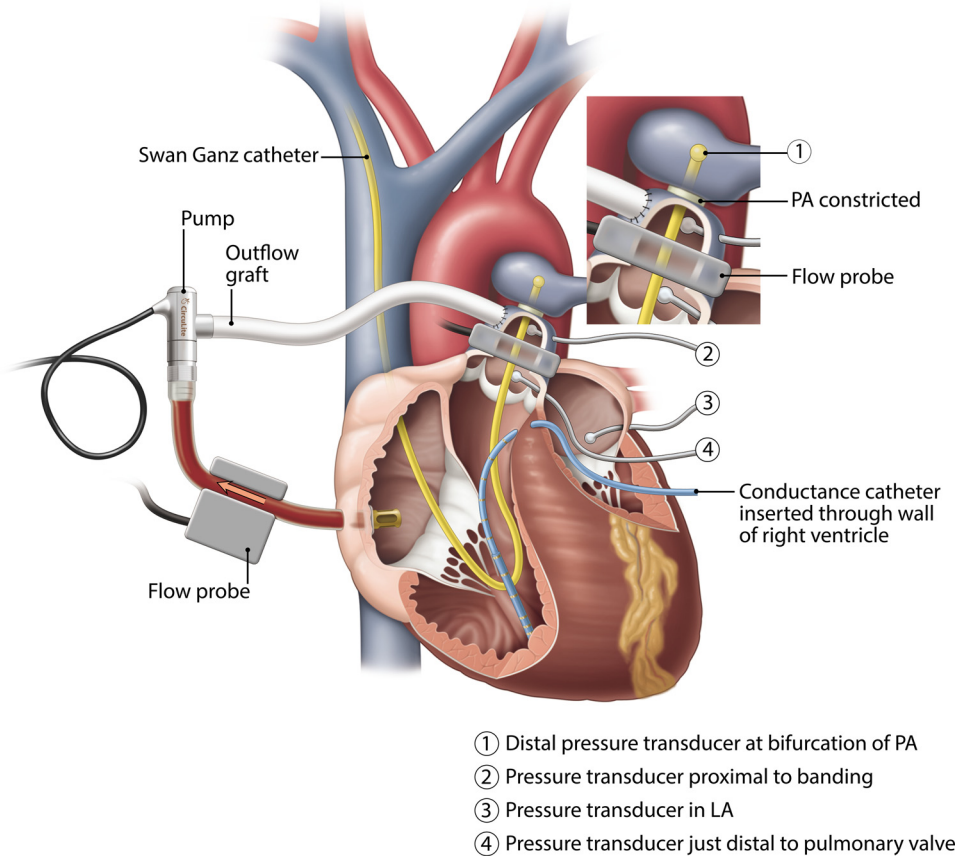

Fig. 1. Schematic overview of the experimental set-up. PA, pulmonary artery. LA, left atrium.

total mechanical energy generated by ventricular contraction and is equal to the sum of SW and the elastic potential energy (PE). PE = ESP (ESV − V_0)/2 − EDP (EDV − V_0)/4, in which ESP is end-systolic pressure, ESV is end-systolic volume, V_0 is theoretical volume when no pressure is generated, EDP is end-diastolic pressure, and EDV is end-diastolic volume. The end-systolic PV-relationship (ESPVR) was determined by using a single beat estimation method by means of a sine curve fitting [A * sin (Bt + C) + D] in which parameters A to D are calculated by the Levenberg-Marquardt procedure in Matlab (2, 16, 26). The Levenberg-Marquardt algorithm iterates through various values of these parameters such that the error (difference between the real function and the computed fitted function) becomes minimal. The two parts of the pressure-time curve surrounding the area where contraction and relaxation were maximal (i.e., dP/dt = max and dP/dt = min, respectively) in the same steady-state heart beat were fitted to the above sine function. P_{max} was the result of the summation of the Levenberg-Marquardt algorithm calculated parameters A and D, and is used in the single beat method to calculate the ESPVR. From this ESPVR the slope (Ees, end-systolic elastance) and volume axis intercept (V_0) were determined. Because both Ees and V_0 varied in different directions of contractility, ESPVR V_{30}, the volume at an end-systolic pressure of 30 mmHg was calculated and served as an additional index of contractility (15). The end-diastolic PV-relationship (EDPVR) was determined using computational single beat methods (3,14). From these curves ($P = \alpha V^{\beta}$), EDPVR V_{20}, the volume at which diastolic pressure equaled 20 mmHg was calculated and served as an index of capacitance. To compare these curves of compliance, the curve-fit expressions were linearized using a logarithmic transformation (ln) of pressure and volume data (15). This resulted in β as slope and in $[-\ln(\alpha)/\beta]$ as V_0. The effective arterial elastance (Ea), indexing the afterload, was calculated as ESP/SV, in which SV is stroke volume.

Data are presented as means ± SD. Statistical analysis was performed using Statistica 10.0 (StatSoft, Tulsa, OK) software. Direct comparisons between baseline states under three conditions and between baseline and RVAD-supported conditions at low flow and at high flow were made using Wilcoxon matched pairs test. A P value of less than 0.05 was considered statistically significant.

RESULTS

Description of three conditions. Hemodynamics and PV-loop parameters of the different conditions before RVAD support are depicted in Tables 1, 2, 3, and 4 and illustrated in Figs. 2, *top left*; 3*A*; and 4*A*.

Banding the PA increased RV afterload (indexed by Ea), which significantly increased RV dimensions (ESV and EDV) and RV pressures (RV peak pressure, ESP, and EDP). The resulting reduction of RV SV and ejection fraction (EF) significantly decreased ABP and CO and significantly increased CVP. LAP did not increase due to better left atrial filling but because of increased dimensions and pressures in the adjacent RV and right atrium. Although the work performed in one heart cycle (SW and PVA) did not increase significantly, the

Table 1. *Pressures and flows*

			Flow	
	n	No Support	Low	High
Baseline	7			
mABP, mmHg		60.0 ± 7.1	66.3 ± 11.2*	66.6 ± 9.4*
mPAP, mmHg		16.1 ± 2.7	16.0 ± 2.3	17.9 ± 2.8″
mCVP, mmHg		8.0 ± 1.2	8.4 ± 1.3	8.3 ± 1.3
Heart rate, beats/min		94 ± 8	89 ± 8*	85 ± 11*″
mLAP, mmHg		4.0 ± 2.2	4.6 ± 2.1	4.9 ± 1.6
Pump flow, l/min		0 ± 0	1.93 ± 0.63*	2.58 ± 0.71*″
RVCO, l/min		3.76 ± 0.56	2.46 ± 0.72*	1.81 ± 0.68*″
Total CO, l/min		3.76 ± 0.56	4.39 ± 1.13	4.39 ± 1.03
Banding	7			
mABP, mmHg		46.7 ± 5.9	56.1 ± 13.3*	55.4 ± 11.6*
mPAP proximal, mmHg		31.4 ± 5.9	39.3 ± 7.2*	44.9 ± 9.4*″
Systolic		51.1 ± 9.2	54.4 ± 9.5*	56.8 ± 9.2*″
Diastolic		20.2 ± 5.3	31.3 ± 7.6*	38.7 ± 10.3*″
mPAP distal, mmHg		15.7 ± 2.9	18.1 ± 2.7*	18.9 ± 3.4*
mCVP, mmHg		13.1 ± 2.0	11.6 ± 2.1*	11.0 ± 2.6*
Heart rate, beats/min		92 ± 9	91 ± 10	90 ± 8
mLAP, mmHg		5.6 ± 1.9	7.0 ± 2.0*	7.9 ± 2.2*
Pump flow, l/min		0 ± 0	1.62 ± 0.56*	2.32 ± 0.70*″
RVCO, l/min		2.51 ± 0.65	1.86 ± 0.40*	1.59 ± 0.33*″
Total CO, l/min		2.51 ± 0.65	3.48 ± 0.84*	3.91 ± 0.82*″
Banding + ischemia	5			
mABP, mmHg		30.2 ±7.4	37.6 ± 6.5*	38.8 ± 6.4*
mPAP proximal, mmHg		24.8 ± 5.8	33.4 ± 5.7*	39.4 ± 6.1*″
mPAP distal, mmHg		15.4 ± 2.9	18.2 ± 2.9	17.6 ± 3.4
mCVP, mmHg		14.6 ± 3.0	14.2 ± 2.6	13.6 ± 2.2
Heart rate, beats/min		69± 11	75 ± 16	77 ± 13
mLAP, mmHg		6.6 ± 1.1	7.8 ± 1.1*	8.4 ± 1.5*
Pump flow, l/min		0 ± 0	1.29 ± 0.35*	1.96 ± 0.48*″
RVCO, l/min		1.30 ± 0.23	0.96 ± 0.33	0.92 ± 0.50
Total CO, l/min		1.30 ± 0.23	2.25 ± 0.25*	2.88 ± 0.61*″

Values are means ± SE. mABP, mean arterial blood pressure; mPAP, mean pulmonary arterial pressure; proximal, just proximal to the band; distal, distal to the band; mCVP, mean central venous pressure; mLAP, mean left atrial pressure; RVCO, right ventricular cardiac output; CO, cardiac output; Underlined values represent statistical significant difference with baseline; double underlined values are statistical significant difference with baseline and banding. *Statistical significant difference with no support;″statistical significant difference with low flow.

Table 2. *PV-loop pressures and volumes*

	n	No support	Flow	
			Low	High
Baseline	7			
Peak RV pressure, mmHg		26.6 ± 4.2	24.9 ± 7.2	26.0 ± 8.8
EDP, mmHg		5.5 ± 1.6	4.8 ± 1.4	4.9 ± 1.9
ESP, mmHg		21.6 ± 5.6	23.0 ± 7.1	24.6 ± 8.3″
EDV, ml		63.1 ± 3.0	52.0 ± 7.3*	47.9 ± 8.3*
ESV, ml		23.9 ± 5.5	25.7 ± 6.3	27.0 ± 7.3*″
SV, ml		39.2 ± 7.0	26.3 ± 10.4*	20.9 ± 10.4*″
EF, %		62 ± 9	49 ± 17*	42 ± 20*″
Banding	7			
Peak RV pressure, mmHg		51.9 ± 7.0	59.4 ± 6.2*	59.8 ± 6.5*
EDP, mmHg		16.1 ± 3.8	16.1 ± 3.8	14.4 ± 3.0*″
ESP, mmHg		49.8 ± 7.0	58.7 ± 4.6*	59.0 ± 5.6*
EDV, ml		100.2 ± 7.1	95.6 ± 7.4*	93.6 ± 8.2*″
ESV, ml		73.1 ± 9.8	75.2 ± 7.8	76.1 ± 8.4
SV, ml		27.2 ± 5.4	20.4 ± 2.8*	17.5 ± 2.7*″
EF, %		27 ± 6	21 ± 3*	19 ± 3*″
Banding + ischemia	5			
Peak RV pressure, mmHg		33.1 ± 3.4	39.0 ± 5.8	39.7 ± 5.9
EDP, mmHg		18.0 ± 5.0	17.1 ± 4.6	17.1 ± 3.5
ESP, mmHg		31.5 ± 3.7	37.9 ± 7.2	39.1 ± 6.7*″
EDV, ml		99.0 ± 12.0	95.0 ± 14.1	94.9 ± 13.1*
ESV, ml		80.4 ± 15.9	81.2 ± 19.3	82.3 ± 19.6
SV, ml		18.6 ± 6.0	13.8 ± 8.7*	12.6 ± 9.0
EF, %		19 ± 7	15 ± 10*	14 ± 11

Values are means ± SE. RV, right ventricular; EDP, end-diastolic pressure; ESP, end-systolic pressure; EDV, end-diastolic volume; ESV, end-systolic volume; SV, stroke volume; EF, ejection fraction. Underlined values are statistical significant difference with baseline; double underlined values are statistical significant difference with baseline and banding. *Statistical significant difference with no support;″statistical significant difference with low flow.

power delivered by the RV in terms of pressures and flows increased significantly. Intrinsic RV contractility was not significantly impacted by PA-banding, evidenced by no significant change in V_{30}. However, the EDPVR shifted rightward and downward with a significant increase of the slope (β) and of V_0 of the linearized EDPVR. RV capacitance (V_{20}) increased significantly. This signifies acute ventricular dilatation in the face of pressure overload.

Unlike with PA-banding alone, RV contractility decreased when ischemia was created (banding + ischemia). RVF worsened, manifested by a further significant increased CVP, further significant decreased ABP and CO, and a significant decreased heart rate. With decreasing RV contractility, RV pressure generating capability decreased causing decreasing PAPs. Because the afterload remained the same (fixed banding), ESV significantly increased and ESP significantly decreased, whereas EDV and EDP remained comparable with the banding condition. Consequently, SV and EF significantly decreased further. SW and RV power decreased significantly compared with baseline and banding conditions. Ventricular capacitance, the slope (β) and the V_0 of the linearized EDPVR remained comparable with the banding condition. Both in band-

Table 3. *Work and power*

	n	No Support	Flow	
			Low	High
Baseline	7			
SW, ml × mmHg		889 ± 578	552 ± 494*	353 ± 280*″
PVA, ml × mmHg		1,196 ± 710	823 ± 600*	584 ± 346*″
RV power,Watt		0.17 ± 0.02	0.11 ± 0.01*	0.08 ± 0.02*
Total power, Watt		0.13 ± 0.02	0.16 ± 0.03	0.18 ± 0.04*
Banding	7			
SW, ml × mmHg		871 ± 328	692 ± 299*	566 ± 330*″
PVA, ml × mmHg		1,928 ± 650	1,513 ± 738	1,236 ± 264*
RV power, Watt		0.17 ± 0.02	0.11 ± 0.01*	0.08 ± 0.02*″
Total power, Watt		0.17 ± 0.02	0.30 ± 0.06*	0.38 ± 0.07*″
Banding + ischemia	5			
SW, ml × mmHg		326 ± 165	309 ± 168	272 ± 192
PVA, ml × mmHg		1,680 ± 1,860	737 ± 535	560 ± 345
RV power, Watt		0.07 ± 0.03	0.06 ± 0.02	0.05 ± 0.02
Total power, Watt		0.07 ± 0.03	0.17 ± 0.04*	0.25 ± 0.07*″

Values are means ± SE. SW, stroke work; PVA, pressure-volume area. Underlined values are statistical significant difference with baseline; double underlined areas are statistical significant difference with baseline and banding. *Statistical significant difference with no support;″statistical significant difference with low flow.

Table 4. *Contractility, relaxation, and ventriculo-arterial coupling*

	n	No Support	Flow	
			Low	High
Baseline	7			
Contractility				
ESPVR; Ees		1.23 ± 1.22	1.30 ± 0.90	2.02 ± 2.03
ESPVR; V_0		−3.7 ± 17.4	2.2 ± 16.1	6.3 ± 17.4
ESPVR; V_{30}		35.5 ± 10.7	34.5 ± 9.6	34.2 ± 9.1
Compliance				
EDPVR; V_{20}		79.9 ± 7.3	67.2 ± 8.6*	62.4 ± 11.6*
ln (EDPVR); β		5.70 ± 0.09	5.66 ± 0.08	5.65 ± 0.14
(EDPVR); V_0		3.9 ± 0.1	3.7 ± 0.01*	3.6 ± 3.2*
Ventriculo-arterial coupling				
Ea		0.56 ± 0.11	1.04 ± 0.61*	1.89 ± 1.96*″
Ees/Ea		2.15 ± 1.97	1.21 ± 0.35	1.08 ± 0.43
Banding	7			
Contractility				
ESPVR; Ees		1.24 ± 0.63	2.29 ± 1.07*	3.04 ± 2.61*
ESPVR; V_0		19.3 ± 41.6	41.4 ± 27.9	47.3 ± 17.7″
ESPVR; V_{30}		54.4 ± 15.3	58.4 ± 18.1	62.3 ± 11.9″
Compliance				
EDPVR; V_{20}		104.5 ± 9.7	99.8 ± 10.4*	99.4 ± 10.0*
ln (EDPVR); β		6.11 ± 0.20	6.11 ± 0.20	6.00 ± 0.10″
ln (EDPVR); V_0		4.2 ± 0.1	4.1 ± 0.1*	4.1 ± 0.1*″
Ventriculo-arterial coupling				
Ea		1.88 ± 0.41	2.91 ± 0.29*	3.41 ± 0.46*″
Ees/Ea		0.65 ± 0.33	0.80 ± 0.40	0.92 ± 0.77
Banding + ischemia	5			
Contractility				
ESPVR; Ees		/0.71 ± 0.50/	1.79 ± 1.11	2.35 ± 1.77*
ESPVR; V_0		−12.3 ± 109.9	50.6 ± 36.5	57.7 ± 31.6*
ESPVR; V_{30}		69.9 ± 29.7	73.5 ± 24.3	76.6 ± 22.2
Compliance				
EDPVR; V_{20}		101.6 ± 14.1	98.2 ± 16.0	97.9 ± 15.2
ln (EDPVR); β		6.56 ± 0.97	6.38 ± 0.79	6.21 ± 0.39
ln (EDPVR); V_0		4.2 ± 0.1	4.1 ± 0.2*	4.1 ± 0.1*
Ventriculo-arterial coupling				
Ea		1.86 ± 0.71	3.82 ± 2.16	5.02 ± 3.42*″
Ees/Ea		0.39 ± 0.31	0.57 ± 0.33	0.56 ± 0.32

Values are means ± SE. ESPVR, end-systolic pressure-volume relationship; Ees, end-systolic elastance; EDPVR, end-diastolic pressure-volume relationship; V_x, volume intercept for a given pressure of × mmHg; Ea, arterial elastance; Ees/Ea, ventriculo-arterial coupling; ln, a logarithmic transformation. Underlined values are statistical significant difference with baseline. /.../Statistical significant difference with banding; *statistical significant difference with no support; ″statistical significant difference with low flow.

ing and banding + ischemia conditions, ventriculo-arterial coupling (indexed by Ees/Ea ratio) significantly decreased compared with the baseline condition.

Mechanical RV support in the baseline condition. Hemodynamics and PV-loop parameters are depicted in Tables 1–4 and illustrated in Figs. 2, *top right*; 3*B*; and 4*B*.

Mechanical support augmented native CO by 44 ± 10% at low flows and by 59 ± 13% at high flows ($P < 0.001$). EDV and heart rate significantly decreased. Peak RV pressures remained constant, but PAP, ESP, and ESV significantly increased at high flows. This was reflected by significant and flow-dependent decreases of SV, EF, SW, and PVA. The decreased heart rate contributed also to the significantly decreased RVCO and RV power. Hence, although ABP significantly increased, total CO did not. Contractility was not influenced. But the EDPVR shifted leftward and slightly upward with a slightly decreased slope (β) and a significantly decreased V_0 of the linearized EDPVR. RV capacitance (V_{20}) decreased significantly.

Mechanical RV support at increased resistance (banding). Hemodynamics and PV-loop parameters are depicted in Tables 1–4 and illustrated in Figs. 2, *bottom left*; 3*C*; and 4*C*.

Mechanical support augmented native CO by 46 ± 8% at low flows and by 59 ± 9% at high flows ($P < 1.10^{-5}$). Peak RV pressure and ESP significantly increased. The decrease of EDV was flow dependent. EDP decreased, only significant at high flows. Consequently, SV and EF significantly decreased. The significant and flow-dependent increase of PAP was mainly determined by increased diastolic pressures and less by modestly increased systolic pressures. A significant and flow-dependent increase of ABP, LAP, total CO, and power was noticed, whereas CVP significantly decreased. PVA decreased as well in a flow-dependent manner. This decrease was only significantly at high flows (low flow: $P = 0.0876$, high flow: $P = 0.0232$). The increasing V_{30} signified a decreased contractility, only statistically significant at high flows. The EDPVR shifted leftward with a decreasing slope (β) and a significantly decreased V_0 of the linearized EDPVR. RV capacitance (V_{20}) decreased significantly.

Mechanical support of the ischemic RV at increased resistance (banding ± ischemia). Two sheep did not survive the coronary artery ligation. Hemodynamics and PV-loop parameters of five sheep are depicted in Tables 1–4 and illustrated in Figs. 2, *bottom right*; 3*D*; and 4*D*.

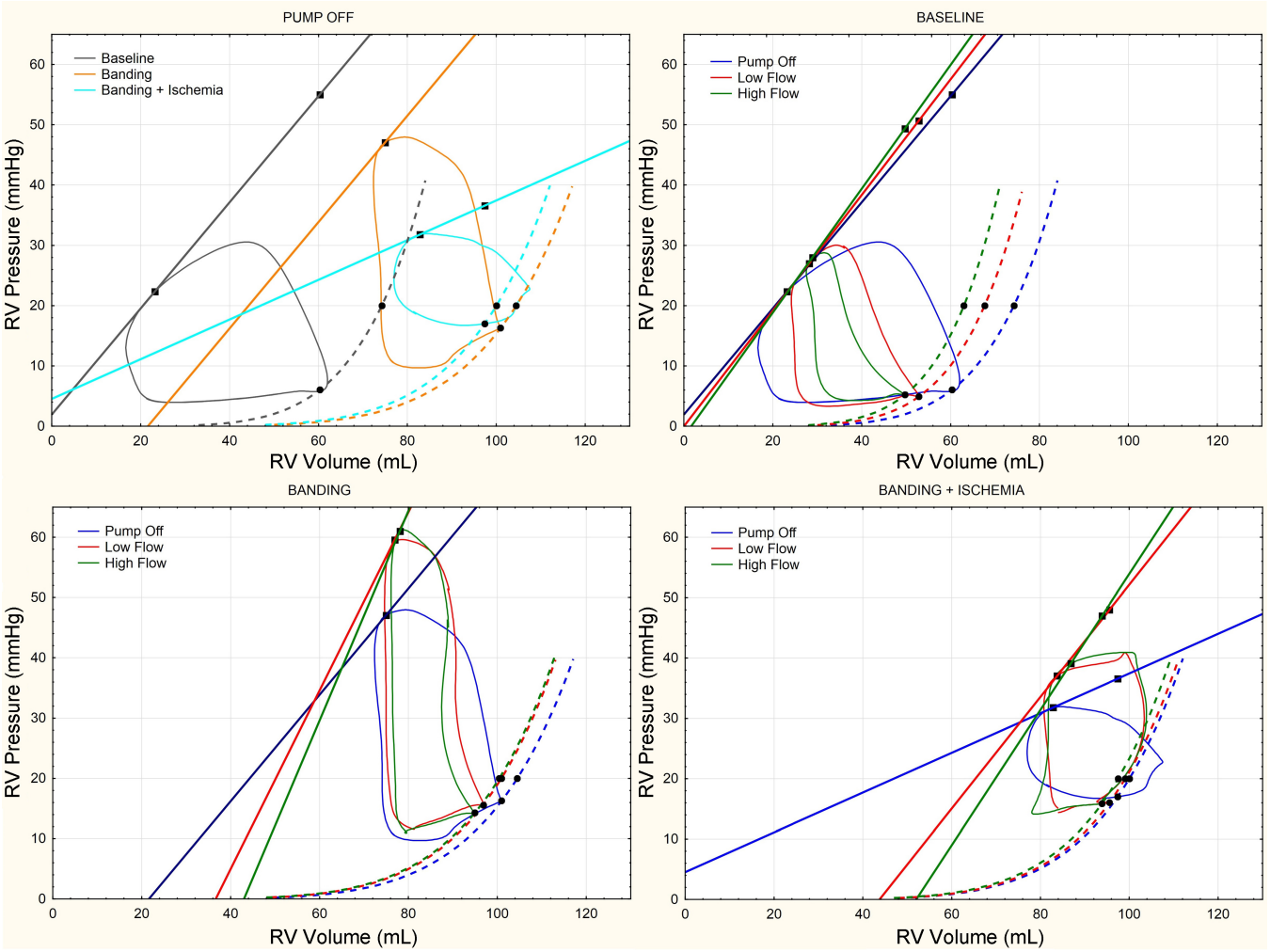

Fig. 2. *Top left*: pressure-volume (PV)-loops of the unsupported right ventricle (RV) in the 3 conditions. *Top right*: PV-loops in the baseline condition. *Bottom left*: PV-loops in the banding condition. *Bottom right*: PV-loops in the banding + ischemia condition. ■, end-systolic point on the PV-loop and maximum pressure point (P_{max}) through which the end-systolic PV relation (ESPVR) is drawn; ●, end-diastolic point on the PV-loop through which the end-diastolic PV relation (EDPVR) is drawn and the point on this EDPVR is at a pressure of 20 mmHg.

Mechanical support augmented native CO by 57 ± 14% at low flows and by 69 ± 13% at high flows ($P < 0.01$). It caused an increased ESP, a decreased EDV (only significant at high flows), and a significant and flow-dependent increased PAP. This was reflected in flow-dependent decreases of SV and EF, only significant at low flows. The increases of ABP, LAP, total CO, and power were significant and flow dependent. Contractility was not modified. The EDPVR slightly shifted leftward with a nonsignificant decrease of the slope (β) and a significantly decreased V_0 of the linearized EDPVR. RV capacitance (V_{20}) decreased significantly.

DISCUSSION

We aimed to test the feasibility and hemodynamic effects of low flow mechanical support of the pressure overloaded RV. The Synergy Micro-pump drove blood from the right atrium to the PA in seven sheep under three different conditions. In all conditions a flow-dependent improvement of CO and CVP was noticed, but also a flow-dependent increase in pulmonary pressures. Intrinsic RV contractility was not significantly impacted, even under ischemic conditions. But RV capacitance successfully decreased.

RVF due to an increased afterload occurs in two populations of adults: *1*) patients with pre-existing chronic pulmonary hypertension in whom the RV went through phases of adaptive hypertrophy and dilatation before clinical failure emerged and *2*) patients with a sudden increase in afterload immediately leading to RVF. Examples of the second group are transplant recipients and patients with acute lung injury or acute respiratory distress syndrome (ARDS) (24). Our animal model mostly mimics the population in this second group.

When RV continuous flow pumps developed for LV support are used, two important issues need to be addressed. First, both these pumps and the RV itself demonstrate a high afterload sensitivity (5, 19). Because the RV normally ejects blood into a low-resistance and high-compliance system, the lower pressure gradient across right-sided VADs could increase flow rates compared with the same devices placed on the left. Such elevated flow rates could lead to elevated PAPs and pulmonary edema or hemorrhage. For the afterload sensitive RV, elevated

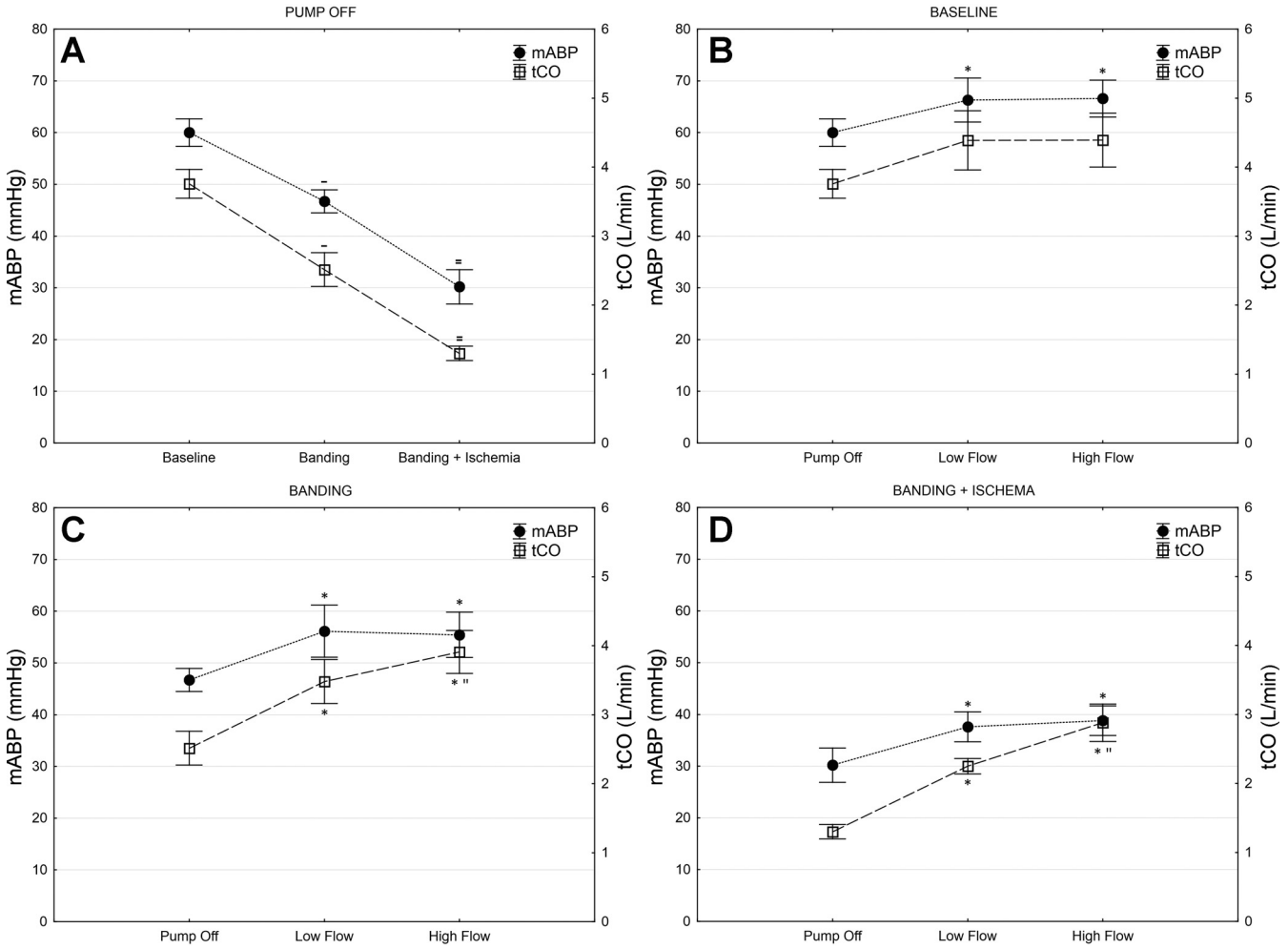

Fig. 3. Parameters of end-organ perfusion. *A*: unsupported RV in the 3 conditions. *B*: baseline condition. *C*: banding condition. *D*: banding + ischemia condition. Underlined values represent statistical significant difference with baseline; double underlined values represent statistical significant difference with baseline and banding. *Statistical significant difference with no support; "statistical significant difference with low flow. mABP, mean arterial blood pressure; tCO, total cardiac output.

PAPs might cause further dilatation and failure. Banding the outflow graft to increase the pressure gradient across the pump has been proposed as a solution (8, 11, 27). Nevertheless, with proper patient selection, e.g., RVF due to an increased afterload, the pressure gradient across right-sided pumps becomes less of a concern. Second, RVADs most probably will be used to support the pressure overloaded RV when the PVR cannot be reduced medically. Therefore, the fear of increasing PAP remains, since increasing total CO in these circumstances will increase PAP as well. To minimize this PAP increase caused by RVADs, and in analogy with the partial support concept for LVADs, we presumed that smaller assist devices with lower flow capacities would be more appropriate for RV support.

The goals of mechanically supporting the pressure overloaded RV are twofold: improving end-organ perfusion (reflected by total CO and ABP) (Fig. 3) and unloading the RV (decreasing peak RV pressure, CVP, PVA, and EDV) (Fig. 4) to improve coronary perfusion and prevent (or even reverse) any maladaptive ventricular remodeling that has occurred.

In the baseline condition, mechanical support induced a flow-dependent RV unloading but no improvement in total CO and ABP. Native RVCO mainly lowered due to decreased heart rates. However, unsupported total CO and ABP in this condition is considered normal. Physiology allows the normal, not fixed, PVR to decrease in response to increased flows. Therefore, PAPs did not increase so extensively compared with the other conditions.

PA-banding has been described to increase RV contractility, whereas intrinsic RV diastolic compliance was not affected (23–25). In our banding condition, intrinsic RV contractility was not affected, whereas RV capacitance increased. However, major differences between these studies as well as with our study exist. In particular, hearts of lambs operate at much higher contractile states. They also have thicker, less compliant walls that are less prone to diastolic dilatation. When compared with closed chest preparations, the absence of pericardial constrain in our study may have led to more extensive diastolic dilatations. Moreover, we reached peak RV pressures of 51 mmHg, which is considerably higher than ± 40 mmHg, reported by others. This indicates a stronger banding, which causes more profound increases of EDV and EDP. Also LV contribution to RV systolic function (ventricular interdependence) diminished by the missing pericardium. Higher RV peak systolic pressures causing higher EDPs have been de-

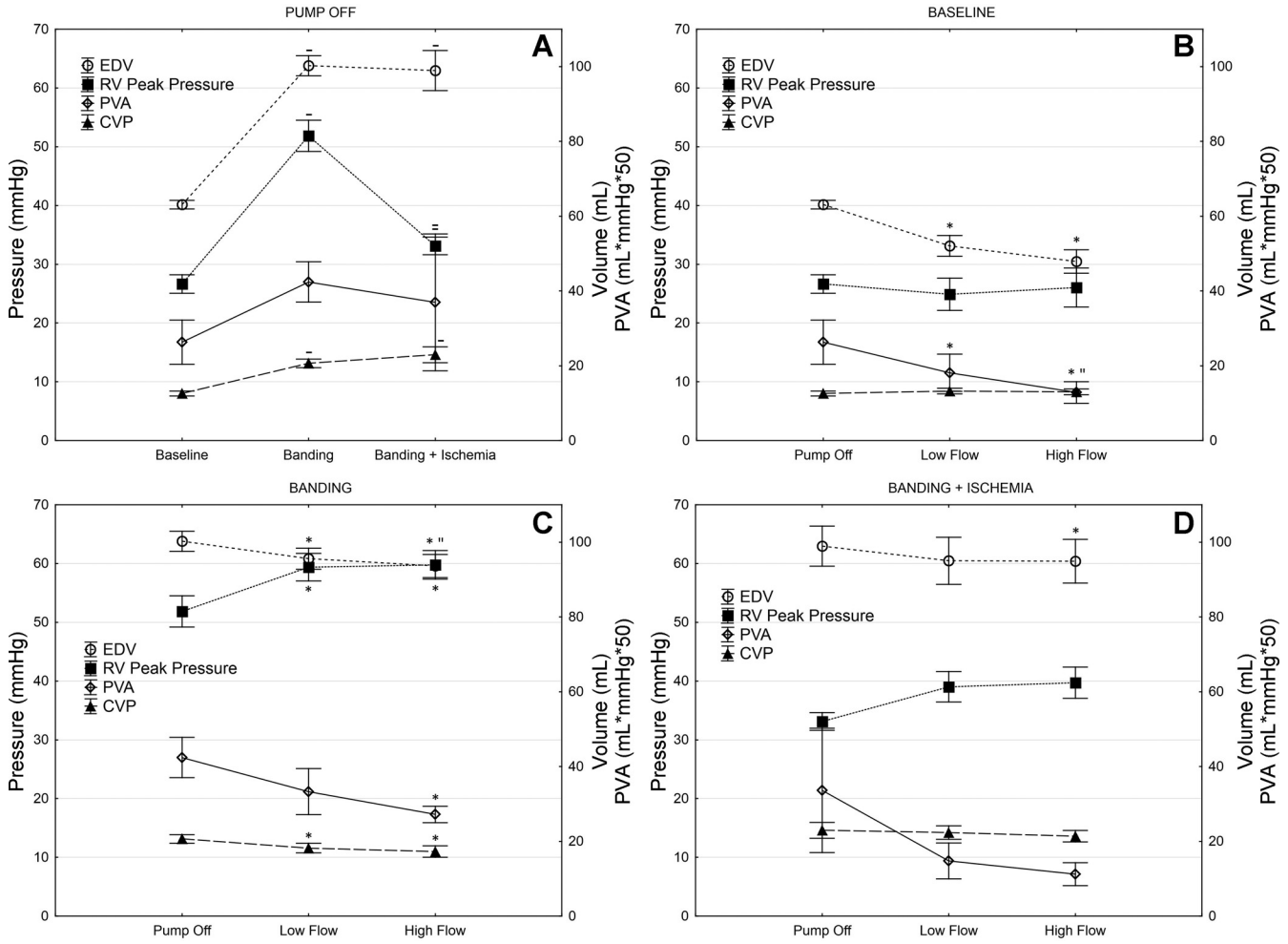

Fig. 4. Parameters of RV unloading. *A*: unsupported RV in the 3 conditions. *B*: baseline condition. *C*: banding condition. *D*: banding + ischemia condition. Underlined values represent statistical significant difference with baseline; double underlined values represent statistical significant difference with baseline and banding. *Statistical significant difference with no support; "statistical significant difference with low flow. EDV, end-diastolic volume; PVA, pressure-volume area; CVP, central venous pressure.

scribed before (25). Together with higher EDVs these indicate a true rightward and downward shift of the EDPVR in our study.

By blood being pumped in the PA, mechanical support induced an increase of RV afterload (indexed by Ea). This reduced native SV. Concomitantly, however, the RV mechanical support used derived blood from the right atrium, thereby reducing RV preload volume and pressure, evidenced by a significantly reduced CVP. This reduced preload causes the SV (and the native RVCO) to decrease further. This had a major influence on the energy expenditure of the RV since both SW and RV power decreased significantly. However, the total delivered right-sided power (RV power + pump power) increased significantly, which is manifested by a significant increase in right-sided total CO. As a consequence, LV filling improved, and this increased total LV CO and LV SV. All these changes were flow dependent. The significantly increased RV peak pressures were caused by the RVAD continuously pumping blood from the right atrium to the PA during diastole, manifested by predominantly increased diastolic PAPs and little increased systolic PAPs (Table 1). This is a potential concern, but increased PAPs were flow dependent as well. Importantly, total CO and ABP at low flows were similar to values measured in the baseline, unsupported condition, and are thus considered sufficient. The significantly leftward shifting EDPVR with its decreased EDP, EDV, and ventricular capacitance indicates a successful diastolic unloading. Because the concomitant increase of systolic pressure afterload was flow dependent and because total CO and ABP at low flow support were considered to be sufficient, we advocate the use of low flow devices to support the pressure overloaded RV.

The nature of our experimental model and of the Synergy Micro-pump imply an imperative opening of the pericardium to band the PA, and to implant the device, respectively. Opening the pericardium will greatly reduce the compressive effect of a dilating RV (and RA) on the LV and left atrium. This will reduce the left-sided filling pressures and per se will already cause better LV CO. However, this will also allow the RV and RA to dilate (and fail) even more than before, causing RV capacitance to further increase and making an RVAD even more beneficial. The difference with catheter-based RVADs that leave the pericardium intact and whether the pericardium should be closed after the device implantation remain the subject for further research.

In heart transplant recipients, preexistent or perioperative pulmonary hypertension and donor organ ischemia contribute to the development of acute refractory RVF (7). Therefore, adding RV ischemia to pressure overload was considered to be clinically relevant. In the banding + ischemia condition, RV support improved ABP and CO, but RV unloading was less convincing. Higher flow rates seemed to be safe and more advantageous. In the clinical situation, ischemic RVs with increased afterload most often have open coronary arteries. In that setting, mechanical support increases ABP and might decrease wall tension, which could improve coronary perfusion (Gregg effect), allowing improvement in contractility and promoting recovery (13). But in our model ischemia is induced by totally occluding the coronary artery. However, the still significant increased CO implies that RVADs might also be beneficial in cases of RV infarction in settings of increased RV afterload. In these circumstances total CO could improve and RVADs might serve as bridge to heart transplantation.

Limitations. First, only a small number of animals was studied. Second, our animal model is not completely clinically representative. The banding is fixed, but PVR is only fixed in end-stage disease. We occluded the coronary artery, while in clinic, ischemia is less absolute and potentially reversible. Finally, we always followed the same sequence: baseline, banding, banding + ischemia. As a result the banding + ischemia group was always studied later and was likely studied from a significantly deteriorated state than the banding alone group.

Conclusions

Mechanical support of the acute pressure overloaded RV improves ABP and CO and provides diastolic unloading of the RV, but with a concomitant and RVAD flow-dependent increase of systolic afterload.

The low flow strategy is potentially beneficial for the afterload sensitive RV and has the advantage of avoiding excessive increases in PAP when pulmonary hypertension exists. This might protect against the development of pulmonary hemorrhage and pulmonary edema. Our data support further research on the use of partial RV support in the chronically pressure-overloaded RV. They also confirm the utility of partial RV mechanical support for RVF in heart transplant patients and in cases of acute lung injury or ARDS.

ACKNOWLEDGMENTS

We thank Ingrid Van Tichelen, Stéphanie De Vleeschauwer, Michael Martin, David Célis, and all the students for valuable help during surgery, the caretaking of the animals, and the handling of the pumps.

GRANTS

This work was supported by a research grant of KULeuven, partially supported by the EU FP7 project SensorArt. CircuLite provided the materials used during surgery.

DISCLOSURES

Daniel Burkhoff is VP Medical Science at Heartware International.

AUTHOR CONTRIBUTIONS

Author contributions: T.V., M.D., F.R., and B.M. conception and design of research; T.V., J.V., M.G., F.R., and B.M. performed experiments; T.V., J.V., and D.B. analyzed data; T.V. and D.B. interpreted results of experiments; T.V. prepared figures; T.V. drafted manuscript; J.V., M.G., D.B., M.D., F.R., and B.M. approved final version of manuscript; D.B., F.R., and B.M. edited and revised manuscript.

REFERENCES

1. **Berman M, Tsui S, Vuylsteke A, Klein A, Jenkins DP.** Life-threatening right ventricular failure in pulmonary hypertension: RVAD or ECMO? *J Heart Lung Transplant* 27: 1188–1189, 2008.
2. **Brimioulle S, Wauthy P, Ewalenko P, Rondelet B, Vermeulen F, Kerbaul F, Naeije R.** Single-beat estimation of right ventricular end-systolic pressure-volume relationship. *Am J Physiol Heart Circ Physiol* 284: H1625–H1630, 2003.
3. **Burkhoff D, Mirsky I, Suga H.** Assessment of systolic and diastolic ventricular properties via pressure-volume analysis: a guide for clinical, translational, and basic researchers. *Am J Physiol Heart Circ Physiol* 289: H501–H512, 2005.
4. **Chen JM, Levin HR, Rose EA, Addonizio LJ, Landry DW, Sistino JJ, Michler RE, Oz MC.** Experience with right ventricular assist devices for perioperative right-sided circulatory failure. *Ann Thorac Surg* 61: 305–310, 1996.
5. **Clark RE, Goldstein AH, Pacella JJ, Walters RA, Moeller FW, Cattivera GR, Davis S, Magovern GJ Sr.** Small, low-cost implantable centrifugal pump for short-term circulatory assistance. *Ann Thorac Surg* 61: 452–456, 1996.
6. **De Vroomen M, Lopes Cardozo RH, Steendijk P, Van Bel F, Baan J.** Improved contractile performance of right ventricle in response to increased RV afterload in newborn lamb. *Am J Physiol Heart Circ Physiol* 278: H100–H105, 2000.
7. **Farrar DJ, Hill JD, Gray LA Jr, Galbraith TA, Chow E, Hershon JJ.** Successful biventricular circulatory support as a bridge to cardiac transplantation during prolonged ventricular fibrillation and asystole. *Circulation* 80: III147–III151, 1989.
8. **Fukamachi K, Shiose A, Massiello AL, Horvath DJ, Golding LA, Lee S, Starling RC.** Implantable continuous-flow right ventricular assist device: lessons learned in the development of a Cleveland Clinic Device. *Ann Thorac Surg* 93: 1746–1752, 2012.
9. **Giesler GM, Gomez JS, Letsou G, Vooletich M, Smalling RW.** Initial report of percutaneous right ventricular assist for right ventricular shock secondary to right ventricular infarction. *Catheter Cardiovasc Interv* 68: 63–66, 2006.
10. **Haddad F, Doyle R, Murphy DJ, Hunt SA.** Right ventricular function in cardiovascular disease. Part II: pathophysiology, clinical importance, and management of right ventricular failure. *Circulation* 117: 1717–1731, 2008.
11. **Hetzer R, Krabatsch T, Stepanenko A, Hennig E, Potapov EV.** Long-term biventricular support with the heartware implantable continuous flow pump. *J Heart Lung Transplant* 29: 822–824, 2010.
12. **Hon JFK, Steendijk P, Khan H, Wong K, Yacoub M.** Acute effects of pulmonary artery banding in sheep on RV pressure-volume relations: relevance to the arterial switch operation. *Acta Physiol Scand* 172: 97–106, 2001.
13. **Klima UP, Guerrero JL, Vlahakes GJ.** Myocardial perfusion and right ventricular function. *Ann Thorac Cardiovas Surg* 5: 74–80, 1999.
14. **Klotz S, Dickstein ML, Burkhoff D.** A computational method of prediction of the end-diastolic pressure-volume relationship by single beat. *Nat Protoc* 2: 2152–2158, 2007.
15. **Klotz S, Hay I, Dickstein ML, Yi GH, Wang J, Maurer MS, Kass DA, Burkhoff D.** Single-beat estimation of end-diastolic pressure-volume relationship: a novel method with potential for noninvasive application. *Am J Physiol Heart Circ Physiol* 291: H403–H412, 2006.
16. **Marquardt D.** An algorithm for least-squares estimation of nonlinear parameters. *SIAM J Imaging Sci* 11: 431–441, 1963.
17. **Meyns B, Klotz S, Simon A, Droogne W, Rega F, Griffith B, Dowling R, Zucker MJ, Burkhoff D.** Hemodynamic response to long-term partial ventricular support with the Synergy pocket micro-pump. *J Am Coll Cardiol* 54: 79–86, 2009.
18. **Morley D, Litwak K, Ferber P, Spence P, Dowling R, Meyns B, Griffith B, Burkhoff D.** Hemodynamic effects of partial ventricular support in chronic heart failure: results of simulation validated with in vivo data. *J Thorac Cardiovasc Surg* 133: 21–28, 2007.
19. **Piazza G, Goldhaber SZ.** The acutely decompensated right ventricle: pathways for diagnosis and management. *Chest* 128: 1836–1852, 2005.
20. **Potapov EV, Loforte A, Weng Y, Jurmann M, Pasic M, Drews T, Loebe M, Hennig E, Krabatsch T, Koster A, Lehmkuhl HB, Hetzer R.**

Experience with over 1000 implanted ventricular assist devices. *J Card Surg* 23: 185–194, 2008.
21. **Price LC, Wort SJ, Finney SJ, Marino PS, Brett SJ.** Pulmonary vascular and right ventricular dysfunction in adult critical care: current and emerging options for management: a systematic literature review. *Crit Care* 14: R169, 2010.
22. **Punnoose L, Burkhoff D, Rich S, Horn EM.** Right ventricular assist device in end-stage pulmonary arterial hypertension: insight from a computational model of the cardiovascular system. *Prog Cardiovasc Dis* 55: 234–243, 2012.
23. **Reiss N, El-Banayosy A, Mirow N, Minami K, Korfer R.** Implantation of the Biomedicus centrifugal pump in post-transplant right heart failure. *J Cardiovasc Surg* 41: 691–694, 2000.
24. **Repessé X, Charron C, Vieillard-Baron A.** Right ventricular failure in acute lung injury and acute respiratory distress syndrome. *Minerva Anestesiol* 78: 941–948, 2012.
25. **Szabo G, Sebening C, Hagl C, Tochtermann U, Vahl CF, Hagl S.** Right ventricular function after brain death: response to an increased afterload. *Eur J Cardiothorac Surg* 13: 449–459, 1998.
26. **Takeuchi M, Igarashi Y, Tomimoto S, Odake M, Hayashi T, Tsukamoto T.** Single beat estimation of the slope of the end-systolic pressure-volume relation in the human left ventricle. *Circulation* 83: 202–212, 1991.
27. **Timms D, Gude E, Gaddum N, Lim E, Greatrex N, Wong K, Steinseifer U, Lovell N, Fraser J, Fiane A.** Assessment of right pump outflow banding and speed changes on pulmonary hemodynamics during biventricular support with two rotary left ventricular assist devices. *Artif Organs* 35: 807–813, 2011.
28. **Yerebakan C, Klopsch C, Niefedt S, Zeisig V, Vollmar B, Liebold A, Sandica E, Steinhoff G.** Acute and chronic response of the RV to surgically induced pressure and volume overload—an analysis of pressure volume relations. *Interact Cardiovasc Thorac Surg* 10: 519–525, 2010.